

---

# A Contrast Sensitive Silicon Retina with Reciprocal Synapses

---

**Kwabena A. Boahen**  
Computation and Neural Systems  
California Institute of Technology  
Pasadena, CA 91125

**Andreas G. Andreou**  
Electrical and Computer Engineering  
Johns Hopkins University  
Baltimore, MD 21218

## Abstract

The goal of perception is to extract invariant properties of the underlying world. By computing contrast at edges, the retina reduces incident light intensities spanning twelve decades to a twentyfold variation. In one stroke, it solves the dynamic range problem and extracts relative reflectivity, bringing us a step closer to the goal. We have built a contrast-sensitive silicon retina that models all major synaptic interactions in the outer-plexiform layer of the vertebrate retina using current-mode CMOS circuits: namely, reciprocal synapses between cones and horizontal cells, which produce the antagonistic center/surround receptive field, and cone and horizontal cell gap junctions, which determine its size. The chip has  $90 \times 92$  pixels on a  $6.8 \times 6.9$ mm die in  $2\mu\text{m}$  n-well technology and is fully functional.

## 1 INTRODUCTION

Retinal cones use both intracellular and extracellular mechanisms to adapt their gain to the input intensity level and hence remain sensitive over a large dynamic range. For example, photochemical processes within the cone modulate the photocurrents while shunting inhibitory feedback from the network adjusts its membrane conductance. Adaptation makes the light sensitivity inversely proportional to the recent input level and the membrane conductance proportional to the background intensity. As a result, the cone's membrane potential is proportional to the ratio between the input and its spatial or temporal average, i.e. contrast. We have

developed a contrast-sensitive silicon retina using shunting inhibition.

This silicon retina is the first to include variable inter-receptor coupling, allowing one to trade-off resolution for enhanced signal-to-noise ratio, thereby revealing low-contrast stimuli in the presence of large transistor mismatch. In the vertebrate retina, gap junctions between photoreceptors perform this function [5]. At these specialized synapses, pores in the cell membranes are juxtaposed, allowing ions to diffuse directly from one cell to another [6]. Thus, each receptor's response is a weighted average over a local region. The signal-to-noise ratio increases for features larger than this region—in direct proportion to the space constant [5].

Our chip achieves a four-fold improvement in density over previous designs [2]. We use innovative current-mode circuits [7] that provide very high functionality while faithfully modeling the neurocircuitry. A bipolar phototransistor models the photocurrents supplied by the outer-segment of the cone. We use a novel single-transistor implementation of gap junctions that exploits the physics of MOS transistors. Chemical synapses are also modeled very efficiently with a single device.

Mahowald and Mead's pioneering silicon retina [2] coded the logarithm of contrast. However, a logarithmic encoding degrades the signal-to-noise ratio because large signals are compressed more than smaller ones. Mead et. al. have subsequently improved this design by including network-level adaptation [4] and adaptive photoreceptors [3, 4] but do not implement shunting inhibition. Our silicon retina was designed to encode contrast directly using shunting inhibition.

The remainder of this paper is organized as follows. The neurocircuitry of the distal retina is described in Section 2. Diffusers and the contrast-sensitive silicon retina circuit are featured in Section 3. We show that a linearized version of this circuit computes the regularized solution for edge detection. Responses from a one-dimensional retina showing receptive field organization and contrast sensitivity, and images from the two-dimensional chip showing spatial averaging and edge enhancement are presented in Section 4. Section 5 concludes the paper.

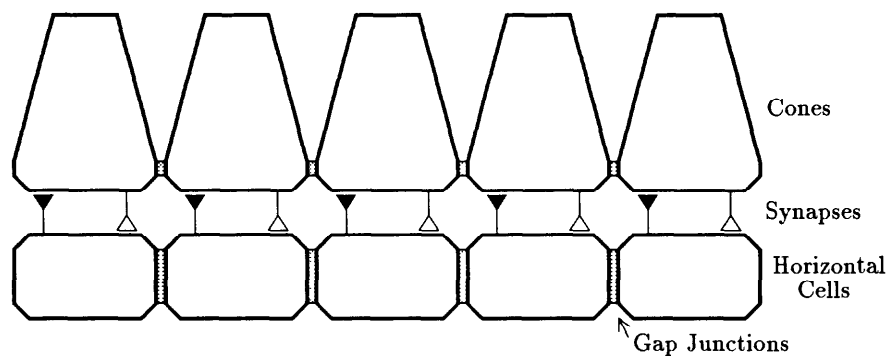


**Figure 1: Neurocircuitry of the outer-plexiform layer. The white and black triangles are excitatory and inhibitory chemical synapses, respectively. The grey regions between adjacent cells are electrical gap junctions.**

## 2 THE RETINA

The outer plexiform layer of the retina produces the well-known antagonistic center/surround receptive field organization first described in detail by Kuffler in the cat [11]. The functional neurocircuitry, based on the red cone system in the turtle [10, 8, 6], is shown in Figure 1. Cones and horizontal cells are coupled by gap junctions, forming two syncytia within which signals diffuse freely. The gap junctions between horizontal cells are larger in area (larger number of elementary pores), so signals diffuse relatively far in the horizontal cell syncytium. On the other hand, signals diffuse poorly in the cone syncytium and therefore remain relatively strong locally. When light falls on a cone, its activity increases and it excites adjacent horizontal cells which reciprocate with inhibition. Due to the way signals spread, the excitation received by nearby cones is stronger than the inhibition from horizontal cells, producing net excitation in the center. Beyond a certain distance, however, the reverse is true and so there is net inhibition in the surround.

The inhibition from horizontal cells is of the shunting kind and this gives rise to contrast sensitivity. Horizontal cells depolarize the cones by closing chloride channels while light hyperpolarizes them by closing sodium channels [9, 1]. The cone's membrane potential is given by

$$V = \frac{g_{Na}E_{Na} + g_D V_{net}}{g_{Na} + g_{Cl} + g_D} \quad (1)$$

where the conductances are proportional to the number of channels that are open and voltages are referred to the reversal potential for chloride.  $g_D$  and  $V_{net}$  describe the effect of gap junctions to neighboring cones. Since the horizontal cells pool signals over a relatively large area,  $g_{Cl}$  will depend on the background intensity. Therefore, the membrane voltage will be proportional to the ratio between the input, which determines  $g_{Na}$ , and the background.

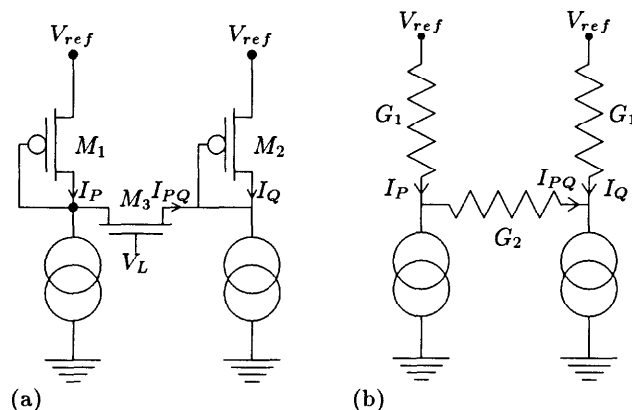


**Figure 2:** (a) Diffusor circuit. (b) Resistor circuit. The diffusor circuit simulates the currents in this linear resistive network.

### 3 SILICON MODELS

In the subthreshold region of operation, a MOS transistor mimics the behavior of a gap junction. Current flows by *diffusion*: the current through the channel is linearly proportional to the difference in carrier concentrations across it [2]. Therefore, the channel is directly analogous to a porous membrane and carrier concentration is the analog of ionic species concentration. In conformity with the underlying physics, we call transistors in this novel mode of operation *diffusors*. The gate modulates the carrier concentrations at the drain and the source multiplicatively and therefore sets the *diffusivity*. In addition to offering a compact gap junction with electronically adjustable ‘area,’ the diffusor has a large dynamic range—at least five decades.

A current-mode diffusor circuit is shown in Figure 2a. The currents through the diode-connected well devices  $M_1$  and  $M_2$  are proportional to the carrier concentrations at either end of the diffusor  $M_3$ . Consequently, the diffusor current is proportional to the current difference between  $M_1$  and  $M_2$ . Starting with the equation describing subthreshold conduction [2, p. 36], we obtain an expression for the current  $I_{PQ}$  in terms of the currents  $I_P$  and  $I_Q$ , the reference voltage  $V_{ref}$  and the bias voltage  $V_L$ :

$$I_{PQ} = e^{\kappa V_L - V_{ref}} (I_Q^{1/\kappa} - I_P^{1/\kappa}) \quad (2)$$

For simplicity, voltages and currents are in units of  $V_T = kT/q$ , and  $I_0$ , the zero bias current, respectively; all devices are assumed to have the same  $\kappa$  and  $I_0$ . The ineffectiveness of the gate in controlling the channel potential, measured by  $\kappa \approx 0.75$ , introduces a small nonideality. There is a direct analogy between this circuit and the resistive circuit shown in Figure 2b for which  $I_{PQ} = (G_2/G_1)(I_Q - I_P)$ . The currents in these circuits are identical if  $G_2/G_1 = \exp(\kappa V_L - V_{ref})$  and  $\kappa = 1$ . Increasing  $V_L$  or reducing  $V_{ref}$  has the same effect as increasing  $G_2$  or reducing  $G_1$ .

Chemical synapses are also modeled using a single MOS transistor. Synaptic inputs to the turtle cone have a much higher resistance, typically  $0.6\text{G}\Omega$  or more [1], than the input conductance of a cone in the network which is  $50\text{M}\Omega$  or less [8]. Thus the synaptic inputs are essentially current sources. This also holds true for horizontal cells which are even more tightly coupled. Accordingly, chemical synapses are modeled by a MOS transistor in *saturation*. In this regime, it behaves like a current source driving the postsynapse controlled by a voltage in the presynapse. The same applies to the light-sensitive input supplied by the cone outer-segment; its peak conductance is about  $0.4\text{G}\Omega$  in the tiger salamander [9]. Therefore, the cone outer-segment is modeled by a bipolar phototransistor, also in saturation, which produces a current proportional to incident light intensity.

Shunting inhibition is not readily realized in silicon because the ‘synapses’ are current sources. However, to first order, we achieve the same effect by modulating the gap junction diffusivity  $g_D$  (see Equation 1). In the silicon retina circuit, we set  $V_L$  globally for a given diffusivity and control  $V_{ref}$  locally to implement shunting inhibition.

A one-dimensional version of the current-mode silicon retina circuit is shown in Figure 3. This is a direct mapping of the neurocircuitry of the outer-plexiform layer (shown in Figure 1) onto silicon using one transistor per chemical synapse/gap junction. Devices  $M_1$  and  $M_2$  model the reciprocal synapses.  $M_4$  and  $M_5$  model

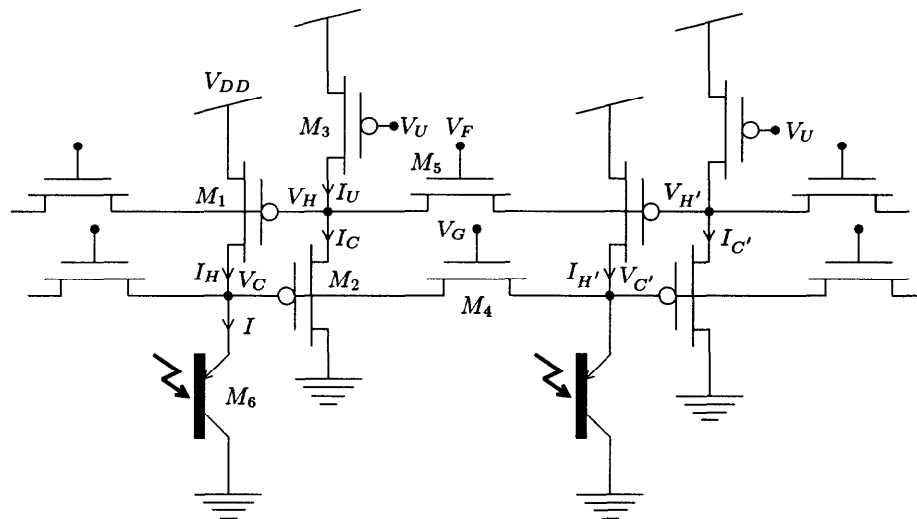


**Figure 3: Current-mode Outer-Plexiform Circuit.**

the gap junctions; their diffusivities are set globally by the bias voltages  $V_G$  and  $V_F$ . The phototransistor  $M_6$  models the light-sensitive input from the cone outer segment. The transistor  $M_3$ , with a fixed gate bias  $V_U$ , is analogous to a leak in the horizontal cell membrane that counterbalances synaptic input from the cone.

The circuit operation is as follows. The currents  $I_C$  and  $I_H$  represent the responses of the cone and the horizontal cell, respectively. These signals are actually in the post-synaptic circuit—the nodes with voltage  $V_C$  and  $V_H$  correspond to the presynaptic signals but they encode the logarithm of the response. Increasing the photocurrent will cause  $V_C$  to drop, turning on  $M_2$  and increasing its current  $I_C$ ; this is excitation.  $I_C$  pulls  $V_H$  down, turning on  $M_1$  and increasing its current  $I_H$ ; another excitatory effect.  $I_H$ , in turn, pulls  $V_C$  up, turning off  $M_2$  and reducing its current  $I_C$ ; this is inhibition.

The diffusors in this circuit behave just like those in Figure 2 although the well devices are not diode-connected. The relationship between the currents given by Equation 2 still holds because the voltages across the diffusor are determined by the currents through the well devices. However, the reference voltage for the diffusors between ‘cones’ ( $M_4$ ) is not fixed but depends on the ‘horizontal cell’ response. Since  $I_H = \exp(V_{DD} - \kappa V_H)$ , the diffusivity in the cone network will be proportional to the horizontal cell response. This produces shunting inhibition.

### 3.1 RELATION TO LINEAR MODELS

Assuming the horizontal cell activities are locally very similar due to strong coupling, we can replace the cone network diffusivity by  $\hat{g} = \langle I_H \rangle g$ , where  $\langle I_H \rangle$  is the local average. Now we treat the diffusors between the ‘cones’ as if they had a fixed

diffusivity  $\hat{g}$ ; the diffusivity in the ‘horizontal cell’ network is denoted by  $h$ . Then the equations describing the full two-dimensional circuit on a square grid are:

$$I_H(x_m, y_n) = I(x_m, y_n) + \hat{g} \sum_{\substack{i = m \pm 1 \\ j = n \pm 1}} \{I_C(x_i, y_j) - I_C(x_m, y_n)\} \quad (3)$$

$$I_C(x_m, y_n) = I_U + h \sum_{\substack{i = m \pm 1 \\ j = n \pm 1}} \{I_H(x_m, y_n) - I_H(x_i, y_j)\} \quad (4)$$

This system is a special case of the dual layer outer plexiform model proposed by Yagi [12]—we have the membrane admittances set to zero and the synaptic strengths set to unity. Using the second-difference approximation for the laplacian, we obtain the continuous versions of these equations

$$I_H(x, y) = I(x, y) + \hat{g} \nabla^2 I_C(x, y) \quad (5)$$

$$I_C(x, y) = I_U - h \nabla^2 I_H(x, y) \quad (6)$$

with the internode distance normalized to unity. Solving for  $I_H(x, y)$ , we find

$$\lambda \nabla^2 \nabla^2 I_H(x, y) + I_H(x, y) = I(x, y) \quad (7)$$

This is the *biharmonic* equation used in computer vision to find an optimally smooth interpolating function ‘ $I_H(x, y)$ ’ for the noisy, discrete data ‘ $I(x, y)$ ’ [13]. The coefficient  $\lambda = \hat{g}h$  is called the regularizing parameter; it determines the trade-off between smoothing and fitting the data. In this context, the function of the horizontal cells is to compute a smoothed version of the image while the cones perform edge detection by taking the laplacian of the smoothed image as given by Equation 6. The space constant of the solutions is  $\lambda^{1/4}$  [13]. This predicts that the receptive field size of our retina circuit will be weakly dependent on the input intensity since  $\hat{g}$  is proportional to the horizontal cell activity.

#### 4 CHIP PERFORMANCE

Data from the one-dimensional chip showing receptive field organization is in Figure 4. As the ‘cone’ coupling increases, the gain decreases and the excitatory and inhibitory subregions of the receptive field become larger. Increasing the ‘horizontal cell’ coupling also enlarges the receptive field but in this case the gain increases. This is because stronger diffusion results in weaker signals locally and so the inhibition decreases. Figure 5(a) shows the variation of receptive field size with intensity—roughly doubling in size for each decade. This indicates a one-third power dependence which is close to the theoretical prediction of one-fourth for the linear model. The discrepancy is due to the body effect on transistor  $M_2$  (see Figure 3) which makes the diffusor strength increase with a power of  $1/\kappa^2$ .

Contrast sensitivity measurements are shown in Figure 5(b). The S-shaped curves are plots of the Michaelis-Menten equation used by physiologists to fit responses of cones [6]:

$$V = V_{max} \frac{I^n}{I^n + \sigma^n} \quad (8)$$

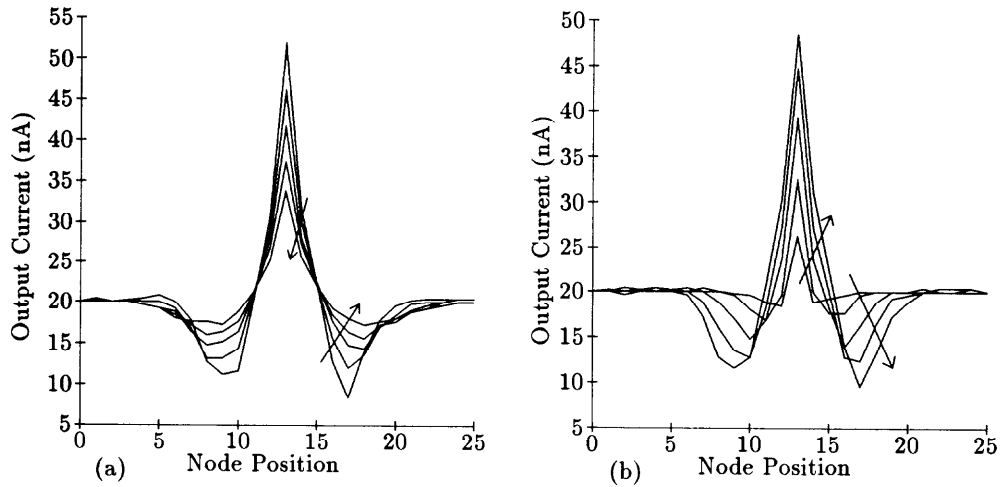


**Figure 4:** Receptive fields measured for  $25 \times 1$  pixel chip; arrows indicate increasing diffusor gate voltages. The inputs were 50nA at the center and 10nA elsewhere, and the output current  $I_U$  was set to 20nA. (a) Increasing inter-receptor diffusor voltages in 15mV steps. (b) Increasing inter-horizontal cell diffusor voltages in 50mV steps.

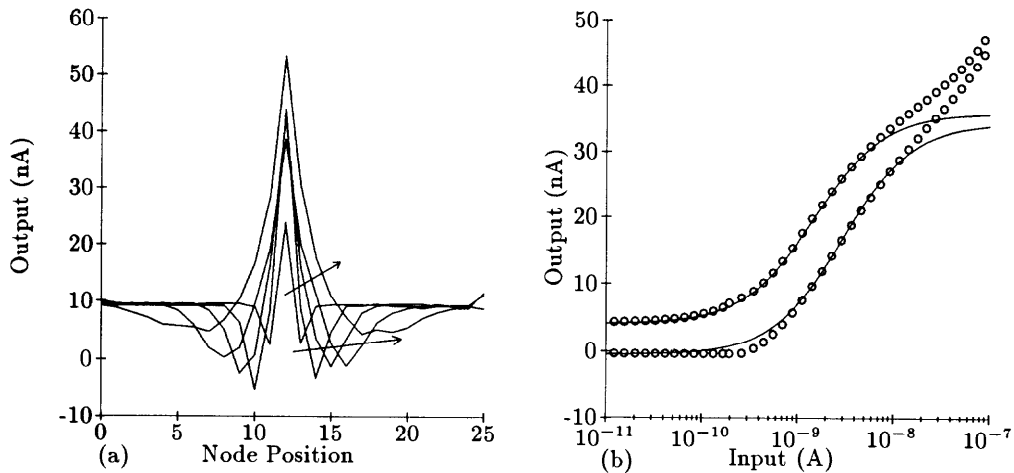


**Figure 5:** (a) Dependence of receptive field on intensity; arrows indicate increasing intensity. Center inputs were 500pA, 5nA, 15nA, 50nA, and 500nA. The background input was always one-fifth of the center input. (b) Contrast sensitivity measurements at two background intensity levels. Lines are fits of the Michaelis-Menten equation.

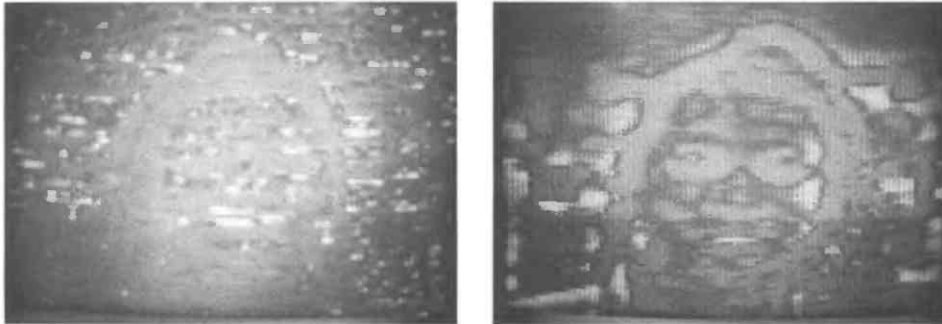


**Figure 6: Video images from  $90 \times 92$  pixel chip with and without cone coupling. The vertical lines between pixels are artifacts of the scanning circuitry.**

where  $\sigma$  is the background intensity and the exponent  $n$  determines the slope of the S-curve. A vertical offset is included to account for the dependence of transistor mismatch on the intensity level. The circuit deviates at high intensities due to increasing inter-receptor coupling strength. For these fits,  $n$  is 1.2 in both cases, compared to the physiologically observed value of 1.0 for cones [6], and  $\sigma$  is 1.5nA and 3.0nA; the actual background intensities were 0.56nA and 1.8nA. Thus the responses are centered at a higher intensity and did not shift horizontally as much as expected with intensity. This is due to the difference in gain for inputs above and below the background level. As the inputs decrease the cone coupling reduces and so the gain increases. Hence there is a smaller range of operation below the background level.

Figure 6 shows video images of a face produced by the two-dimensional silicon retina chip. The chip includes scanning circuitry which rasterizes the image and generates all the signals required to drive a multiscan monitor [14]. The image on the left shows a considerable amount of spatial noise due to transistor mismatch. The face is hardly recognizable. In the other image the inter-cone diffusors have been turned on and greatly enhance the signal-to-noise. The center-surround processing highlights edges, producing the 'halo' around her head, and regions with high curvature, like the cheeks.

## 5 CONCLUSIONS

Using a current-mode approach, we have built a dense, robust, contrast-sensitive silicon retina modeled closely after the vertebrate retina. Our single-transistor gap junctions and chemical synapses yield very efficient implementations of neural networks. Unfortunately, the implementation of shunting inhibition used here makes the receptive fields enlarge with increasing intensity. We are presently developing new circuits that address this problem.



### Acknowledgements

We are very grateful to Carver Mead for his support and encouragement. KB is supported by a graduate fellowship from Caltech. AA is supported by a Research Initiation Award from NSF (MIP-9010364). KB thanks Tobi Delbrück, Andy Moore, Lloyd Watts, Misha Mahowald, and Xavier Arreguit for their help. Chip fabrication was provided by MOSIS and computing facilities in the Mead Lab by Hewlett-Packard.

### References

- [1] A. Kaneko, T. Ohtsuka et.al., "GABA Sensitivity in Solitary Turtle Cones," in *Neurocircuitry of the Retina: A Cajal Memorial*, pp. 89-97, A. Gallego and P. Gouras, Eds, Elsevier, New York NY, 1985.
- [2] C. A. Mead, *Analog VLSI and Neural Systems*, Addison-Wesley, Reading MA, 1989.
- [3] T. Delbrück and C. A. Mead, "An electronic Photoreceptor sensitive to small changes in Intensity," in *Advances in Neural Information Processing Systems I*, D. S. Touretsky ed. Morgan Kaufman , San Mateo CA, 1989.
- [4] M. A. Mahowald, "Silicon Retina with Adaptive Photoreceptors," in *SPIE/SPSE Symposium on Electronic Science and Technology: From Neurons to Chips*. Orlando, FL, April 1991.
- [5] T. D. Lamb and E. J. Simon, "The Relation between Intercellular Coupling and Electrical Noise in Turtle Photoreceptors," *J. Physiol.*, 263, pp. 257-286, 1976.
- [6] J. E. Dowling, *The Retina: An Approachable part of the Brain*, Harvard University Press, Cambridge MA, 1987.
- [7] A. G. Andreou et.al., "Current-Mode Subthreshold MOS Circuits for Analog VLSI Neural Systems," *IEEE Trans. on Neural Networks*, vol. 2, no. 2., pp. 205-213, March 1991.
- [8] P. B. Detwiler and A. L. Hodgkin, "Electrical Coupling between Cones in the Turtle Retina," *J. Physiol.*, 291, pp. 75-100, 1979.
- [9] D. Attwell, F. S. Werblin et. al., "The Properties of Single Cones isolated from the Tiger Salamander Retina," *J. Physiol.*, 328, pp. 259-283, 1982.
- [10] D. A. Baylor, M. G. F. Fourtes et. al., "Receptive Fields of Cones in the Retina of the Turtle," *J. Physiol.*, 214, pp. 265-294, 1971.
- [11] S. W. Kuffler, "Discharge Patterns and Functional Organization of Mammalian Retina," *J. Neurophysiol.*, 16, pp. 37-68, 1953.
- [12] T. Yagi, Y. Funahashi, and F. Ariki, "Dynamic Model of Dual Layer Neural Network for Vertebrate Retina," *Proceedings of IJCNN-89*, Washington DC, June 1989.
- [13] T. Poggio, H. Voorhees, and A. Yuille, "A Regularized Solution to Edge Detection," Massachusetts Institute of Technology, AI Lab Memo 833, May 1985.
- [14] C. A. Mead and T. Delbück, "Scanners for use in visualizing analog VLSI circuitry," *in press*, 1992.